Natural Resources for Human Health

visaga publishing house

Original Research

View Article Online

Check for updates

Received 05 November 2021
Revised 23 December 2021
Accepted 24 December 2021
Available online 07 January 2022

Edited by Balamuralikrishnan Balasubramanian

KEYWORDS:
Characterization
Conjugated silver nanoparticles
Rate of killing
Clinical bacterial isolates

Natr Resour Human Health 2022; 2 (3): 343-348
https://doi.org/10.53365/nrfhh/145339
eISSN: 2583-1194

Characterization and rate of killing of conjugated silver nanoparticles against selected clinical bacterial isolates

Stephen Dare Oloninefa [1, 2,*], Abalaka Moses Enemaduku [2], Daniyan Safiya Yahaya [2], Mann Abdullahi [3]

[1]Department of Quality Control, Jesil Pharmaceutical Industries Limited, Plot No. 15, MTP 54, Industrial Layout, Sauka-Kahuta, Minna, Niger State - 920211, Nigeria
[2]Department of Microbiology, Federal University of Technology, Minna, Niger State, Nigeria
[3]Department of Chemistry, Federal University of Technology, Minna, Niger State, Nigeria

ABSTRACT: The menace of drug resistance, bioavailability and drug delivery to the target sites has motivated researchers to search for new antimicrobial agents from medicinal plants and subsequently use them for the biosynthesis of silver nanoparticles for effective killing of bacteria challenging to kill using crude extracts. The biosynthesis of silver nanoparticles was done using aqueous extract (AQE) of *Euphorbia heterophylla*, while characterization and the killing rate of conjugated silver nanoparticles (CAgNPs) were carried out using standard methods. The maximum wavelength obtained for CAgNPs was 410.33 nm, while the size distribution was 237.8 d.nm. The Fourier Transform Infra-Red result showed O-H (3308.94 cm^{-1}), which is responsible for stabilising and reducing silver ions, while the Transmission Electron Microscopy revealed the presence of monodispersed spherical shapes CAgNPs. The Energy Dispersive Spectroscopy confirmed the presence of silver. There were reductions in the clinical bacterial isolates exposed to CAgNPs as the exposure time increased. *Escherichia coli* was killed between 6-7 h while *Salmonella typhimurium* was killed at the seven has the value of 0.00 log_{10} CFU/ml was recorded respectively. However, there were increments in the populations of clinical bacterial isolates in control as the time of exposure increased. Therefore, the study suggests that the CAgNPs exhibit intense antimicrobial activity and the potential to be developed as an alternative agent to treat bacterial infections, curb multidrug-resistant bacterial infection, and promote speedy drug delivery to the target sites.

1. INTRODUCTION

The daily increase in life-threatening infections caused by multi-resistant microorganisms (especially bacteria) leading to an increase in deaths globally has inspired many researchers to search for antimicrobial agents to develop new antibiotics from medicinal plants (Basappa et al., 2013; Betts et al., 2018). Medicinal plants contain phytochemicals in a crude form that, when biosynthesized into nanoparticles, may exert better therapeutic effects. Medicinal plants' eco-friendliness and cost-effectiveness have increased their popularity for the biological synthesis of silver nanoparticles and nanomaterials (Aritonang et al., 2019). Plant-mediated nanoparticle synthesis is gaining popularity due to the high reactivity of plant extracts and the ease with which plant materials are available. In a comparative toxicity study conducted *in vitro* and *in vivo* (Kalaichelvan et al., 2013), it has been concluded that biologically conjugated AgNPs are less toxic than chemically conjugated AgNPs. This method of nanoparticles synthesis involves no toxic chemicals and has been termed as green chemistry procedure as opined by (Kalaichelvan et al., 2013).

In the post-antibiotic era, research on AgNPs and other nanomaterials has increased in order to identify new agents capable of combating pathogenic microorganisms without promoting the emergence of new resistances (Betts et al., 2018). AgNPs have attracted the attention of researchers and industry due to their exceptional antibacterial activity. Antimicrobial activity of AgNPs has been demonstrated against a variety of infectious and pathogenic microorganisms, including multidrug-resistant bacteria (Siddiqi et al., 2018). AgNPs' potential and usefulness as antibiotic alternatives, as well as their efficacy against multidrug-resistant organisms, are attributed to their diverse modes of action, which attack germs in many structures simultaneously and enable them to kill a variety of bacteria (Cheng et al., 2016; Lee et al., 2019). The infections caused by antibiotic-resistant microorganisms have

* Corresponding author.
E-mail address: dami4nefa2013@gmail.com (Stephen Dare Oloninefa)

profound public health implications and are a global concern. Therefore, the emergence of AgNPs as a viable alternative has been advantageous because they may be used to prevent illnesses caused by these microbes, sanitise medical supplies, and even combat infections during their course. (Betts et al., 2018; Natan & Banin, 2017). This study focuses on the characterization and rate of killing conjugated silver nanoparticles against selected clinical bacterial isolates.

2. MATERIALS AND METHODS

2.1. Collection, Identification and Confirmation of Clinical Bacterial Isolates

The microorganisms used were received from the General Hospital's Microbiology Department. They were Gram-stained, and biochemical tests were performed to confirm their identity using the methods of Cheesbrough (2010). They were then subcultured into Nutrient Agar slants for molecular analysis (B. Incorporation, 2012; B.C. Incorporation, 2016; NCBI, 1988) and kept in a refrigerator until they were ready for further use.

2.2. Biosynthesis of Silver Nanoparticles from Aqueous Crude Extract of Whole Plant of *E. heterophylla*

The biosynthesis of silver nanoparticles from the aqueous crude extract of the whole plant of *E. heterophylla* was carried as outlined in the modified method of Kasthuri et al. (2009). The stock solution of 80 mg/ml was prepared from the aqueous crude extract of the whole plant of *E. heterophylla*. A 0.5 ml aliquot was measured from the stock solution and added to 2.5 ml of 1 mM $AgNO_3$ solution in a test tube, then buffered to the various pH levels of 4, 5, 6, 7, 8, 9, 10 and 11. It was stabilized using 600 molecular weight of poly ethylene glycol (PEG 600) and then made up to the final volume of 5 ml with NaOH and HCl solutions buffers. The test tubes were covered with aluminium foil to avoid photoreduction of silver ions and then incubated at 37°C under agitation (200 rpm) and dark condition for 36 h. In silver nanoparticle formation, the solution turned from yellowish to bright yellow and dark brown.

2.3. Characterization of Conjugated Silver Nanoparticles

2.3.1 Ultraviolet-Visible Spectroscopy of Conjugated Silver Nanoparticles

The ultraviolet-visible spectroscopy of the CAgNPs was determined from 300-700 nm using a UV-Visible Spectrophotometer 20D, Techmel and Techmel, USA (Kasthuri et al., 2009).

2.3.2 Size Distribution of Conjugated Silver Nanoparticles

The size distribution of the CAgNPs was determined using Malvern Zetasizer version 7.01.

2.3.3 Fourier Transform Infra-Red (FT IR) Spectroscopy

The analysis of the functional group of the bio-reducing agent present in the extract (80 mg/ml) was measured by FTIR. A small aliquot of the concentrated reaction mixture was measured in the transmittance mode at 500 to 4500 cm^{-1} after the reaction. The extract spectra were taken after the biosynthesis of silver nanoparticles was determined (Sermakkani & Thangapandian, 2012).

2.3.4 Energy dispersive spectroscopy (EDS)

The energy dispersive X-ray spectrometry carried out an elemental compositional analysis on the sample (EDS) attached with Scanning Electron Microscope (SEM) Machine. THE SEM MACHINE SERVED the EDS analysis of the Ag sample (Sermakkani & Thangapandian, 2012).

2.3.5 Transmission electron microscope (TEM)

To determine the shape and surface morphology, TEM was utilised. Thin films of the sample (conjugated AgNPs solution) were prepared by placing a minimal amount on the carbon-coated grids. The films on the TEM grids were allowed to stand for 2 minutes, and the extra solution was removed using blotting paper, and the grid was then allowed to dry overnight before the measurement was taken. The TEM measurements were carried out on a JEOL model 1200EX instrument, operated at an accelerating voltage at 120 kV (Sermakkani & Thangapandian, 2012).

2.4. Microbiological activity

2.4.1 Standardization of Clinical Bacterial Isolates

The population of clinical isolates was determined using the 0.5 McFarland Turbidity Standard (Mcfarland, 1907; Murray et al., 2007).

2.4.2 Determination of the Rate of Killing

The rate of killing of the CAgNPs and control (without CAgNPs) against the clinical bacterial isolates was determined by the modified method of Hugo and Russell (2000); Oloninefa et al. (2020). A standardized overnight culture with a 1.5 × 108 cfu/ml population was used. A 0.20 ml of the inoculum was added to 10 ml of the conjugated AgNPs. A 1.0 ml of the mixture was withdrawn at intervals of 1, 2, 3, 4, 5, 6 and 7 h respectively and diluted tenfold (10^{-1}), then plated on Mueller Hilton Agar in duplicates incubated at 37°C for 24 h. The rate of killing the clinical bacterial isolates by the control was determined by adding 0.20 ml of the inoculum to 10 ml of Nutrient Broth. A 1.0 ml of the mixture was withdrawn at intervals of 1, 2, 3, 4, 5, 6 and 7 h respectively and diluted tenfold (10^{-1}), then plated on Mueller Hilton Agar in duplicates incubated at 37°C for 24 h. The population of the clinical isolates was counted and expressed in $\log_{10}$ CFU/ml after the exposure to the CAgNPs and control, respectively.

2.5. Data Analysis

The data obtained from the study were subjected to analysis of variance (ANOVA) using IBM SPSS Statistics Version 23 and Microsoft Excel 2010. All data were expressed as mean

± standard error of the mean. The values with different superscripts along the same column were significantly different ($P < 0.05$).

3. RESULTS

3.1. Biochemical characteristics of the clinical isolates

The Gram stain and biochemical assays performed on the four clinical bacterial isolates yielded the following results in Table 1. To identify the isolates, tests for triple sugar iron (TSI), methyl red, indole, catalase citrate utilisation, and urease were performed. The organisms identified and later confirmed by molecular characterization were: *E. coli* strain MRE 600 (CP014197.1), *S. enteric* subsp. enteric serovar typhi PMO 16/13 (CP12091.1), *K. pneumoniae* strain HZW25 (CP025211.1) and *P. fluorescens* strain 2P24 (CP025542.1) (Table 2).

Table 1
Gram reactions and biochemical characteristics of the clinical b acterial isolates

Tests	A	B	C	D
Gram Reactions	-	-	-	-
TSI	A/A, G (+), H_2S (-)	K/A, G (+), H_2S (+)	A/A, G (+), H_2S (-)	K/K, G (-), H_2S (-)
Methyl Red	+	-	+	-
Indole	+	-	-	-
Catalase	+	+	+	+
Citrate Utilisation	-	+	-	+
Urease	+	+	-	+
Identity	*E. coli*	*S. typhimurium*	*K. pneumoniae*	*P. fluorescens*

+ = Positive; - = Negative; TSI= Triple Sugar Iron; K= Alkaline; A= Acid; G= Gas; H_2S= Hydrogen sulphide

Table 2
Molecular Characterization of Clinical Bacterial Isolates

Clinical Isolates	Max Score	Total Score	Query Cover	Expected Value	Identity	Accession Number
E. coli strain MRE 600	2660	16064	100%	0.0	100%	CP014197.1
P. fluorescens strain 2P24	2689	2689	100%	0.0	100%	CP025542.1
Salmonella enteric subsp. enteric serovar typhi PMO 16/13	3546	3546	100%	0.0	100%	CP12091.1
K. pneumoniae strain HZW25	797	6348	100%	0.0	98%	CP025211.1

3.2. UV/Visible Spectrophotometry of Conjugated Silver Nanoparticles

The result of UV/Visible spectrophotometry of conjugated silver nanoparticles determined between pH 4-11 is shown in Table 3. The maximum wavelength obtained was 410.33 nm, while the absorbance value ranges from 0.5333-0.986.

Table 3
UV/Visible Spectrophotometry of Conjugated Silver Nanoparticles

pH	Wavelength	Absorbance
4	410.33 ± 0.333^a	0.533 ± 0.003^a
5	410.33 ± 0.333^a	0.774 ± 0.003^c
6	410.33 ± 0.333^a	0.821 ± 0.005^d
7	410.33 ± 0.333^a	0.711 ± 0.005^b
8	410.33 ± 0.333^a	0.923 ± 0.012^e
9	410.33 ± 0.333^a	0.986 ± 0.003^f
10	410.00 ± 0.333^a	0.975 ± 0.003^f
11	410.33 ± 0.333^a	0.779 ± 0.005^c

Results represent mean ± standard error of the mean of triplicate determination. The values with the same superscript in the same column are not significantly different at p<0.05

3.3. Size Distribution of Conjugated Silver Nanoparticles

Figure 1 shows the size distribution of the CAgNPs. The CAgNPs had a Zeta-average of 237.8 d.nm.

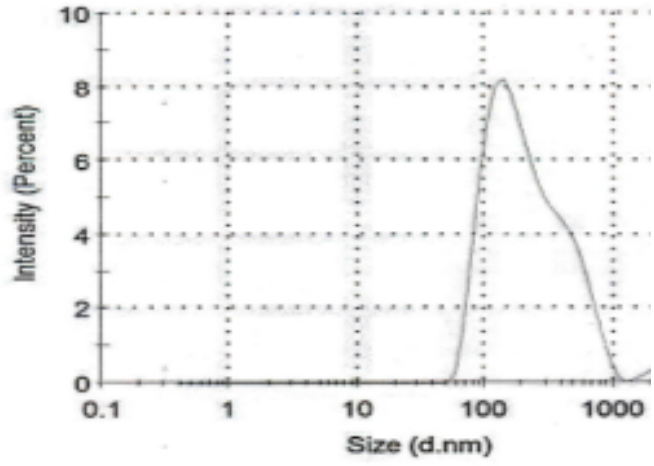

Figure 1. Size Distribution of Conjugated AgNPs. Conjugated AgNPs-Aqueous extract of whole plant of Euphorbia heterophylla + 1mM Silver nitrate solution + PEG 600 (Zeta average = 237.8 d.nm)

3.4. Fourier Transform-Infra Red of Conjugated Silver Nanoparticles

The results of FTIR spectra in Figure 2 reveal the biomolecules responsible for the stability and reduction of silver ions exposed to the aqueous extract of the whole plant of *Euphorbia heterophylla*. The FTIR spectra reveal the peaks at 1635.66 cm-1 and 3308.94 cm-1 which correspond to alkenes (C=C) and alcohol (O-H).

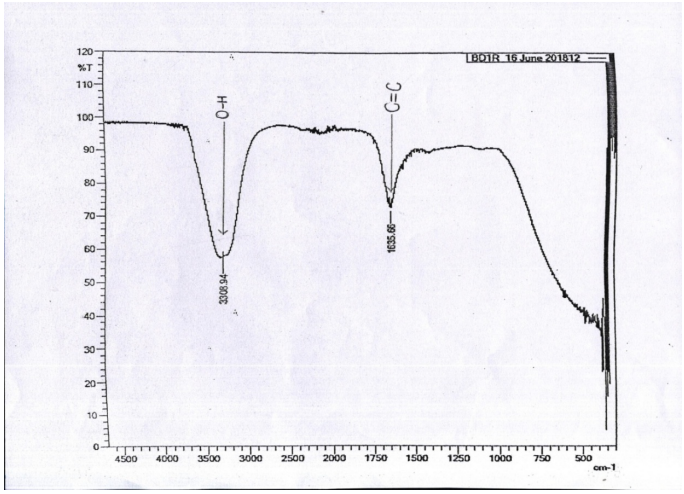

Figure 2. Transform-Infrared Spectroscopy of CAgNPs

3.5. Transmission Electron Microscopy of Conjugated Silver Nanoparticles

Figure 3 show the morphology of the CAgNPs at 50 nm. The CAgNPs were monodispersed and spherical.

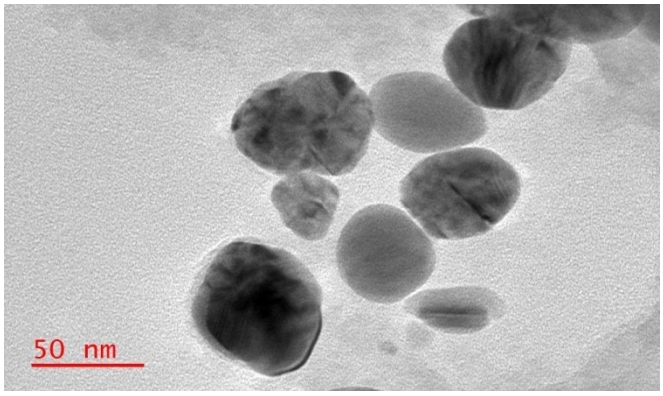

Figure 3. Transmission Electron Microscopy of CAgNPs

3.6. Energy Dispersive Microscopy (EDS) of CAgNPs

Figure 4 shows that CAgNPs contained silver and had 3.0 keV of silver when the EDS was carried out. The presence of carbon and copper in the spectra was part of the materials used during the sample preparation.

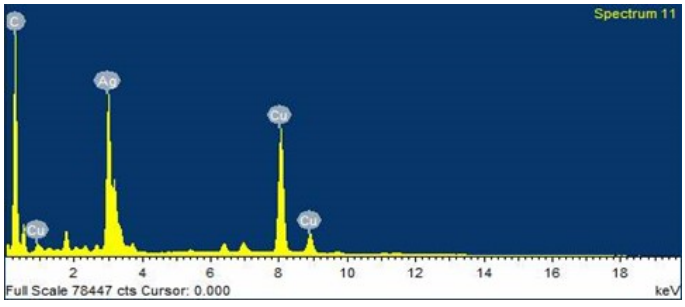

Figure 4. Energy Dispersive Spectroscopy of Conjugated AgNPs

3.7. Rate of Killing

Figure 5 shows the results of the rate of killing of CAgNPs and control when clinical bacterial isolates: *E. coli* strain MRE 600 (CP014197.1), *Salmonella enteric* subsp. Enteric serovar typhi PMO 16/13 (CP12091.1), *K. pneumoniae* strain HZW25 (CP025211.1) and *P. fluorescens* strain 2P24 (CP025542.1) were exposed for 7 h. There was a reduction in the *E. coli* strain MRE 600 (CP014197.1) population from 2.00-1.31$\log_{10}$cfu/ml when exposed to CAgNPs between 1-5 h while 0.00$\log_{10}$cfu/ml was obtained between 6-7 h. There was an increase in the *E. coli* strain MRE 600 (CP014197.1) population from 11.39-14.64$\log_{10}$cfu/ml when exposed to the control for 1-7 h. On the other hand, a reduction in populations of *Salmonella enteric* subsp. enteric serovar typhi PMO 16/13 (CP12091.1) from 2.18-1.49$\log_{10}$cfu/ml was recorded between 1-6 h but 0.00$\log_{10}$cfu/ml was obtained for 7 h when exposed to CAgNPs. However, an increment in the populations of *Salmonella enteric* subsp. Enteric serovar typhi PMO 16/13 (CP12091.1) from 10.96-12.46$\log_{10}$cfu/ml was obtained when exposed to the control for 1-7 h (Figure 5).

Furthermore, there was a reduction in the populations of *K. pneumoniae* strain HZW25 (CP025211.1) from 11.67-11.10$\log_{10}$cfu/ml when exposed to CAgNPs between 1-7 h, while there was an increase in the populations of *K. pneumoniae* strain HZW25 (CP025211.1) from 11.72-11.98$\log_{10}$cfu/ml when exposed to the control for 1-7 h. In addition, there was a reduction in the populations of *P. fluorescens* strain 2P24 (CP025542.1) from 3.13-2.52$\log_{10}$cfu/ml when exposed to CAgNPs between 1-7 h. On the other hand, increment in the populations of *P. fluorescens* strain 2P24 (CP025542.1) from 10.59-11.56$\log_{10}$cfu/ml was recorded when exposed to the control for 1-7 h (Figure 5).

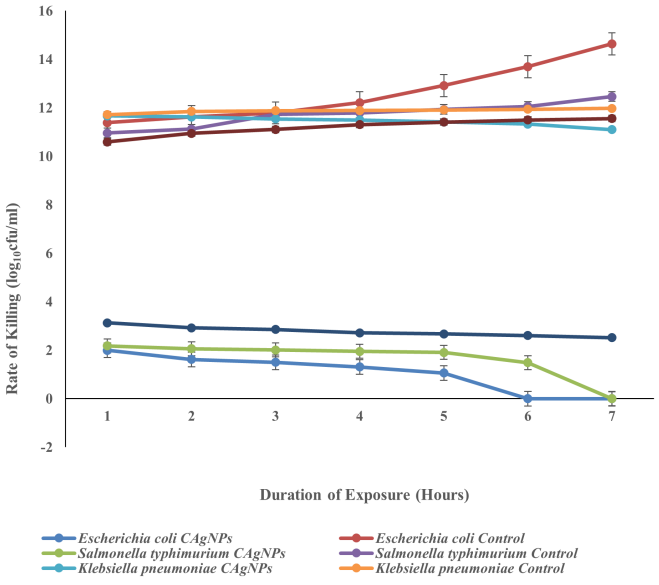

Figure 5. Rate of Killing of Conjugated Silver Nanoparticles and Control

4. DISCUSSION

The maximum wavelength obtained (410.33 nm) when ultraviolet-visible spectroscopy of conjugated silver nanoparticles was determined in line with the studies carried out by Kasthuri et al. (2009); Malawong et al. (2021), which obtained similar results (Table 2). The size distribution of CAgNPs revealed an average size of 237.8 d.nm and was confirmed by the TEM image shown in Figure 3. As opined by Xueting et al. (2018), the size of nanoparticles pave the way for easy penetration of silver ions into the bacterial cell and react with DNA molecule leading to the collapse of DNA replication which eventually causes bacterial cell dysfunction. The result of the FTIR spectrum showing the presence of peak 3308.94 cm^{-1} (O-H) may be responsible for stabilising and reducing the silver ions when exposed to the aqueous extract of the whole plant of *E. heterophylla* during biosynthesis of silver nanoparticles (Figure 2). Meanwhile, the FTIR result obtained disagrees with the works of Govindaraju et al. (2010) as the FTIR spectrum of the plain *S. torvum* leaf extract characterized showed peaks at 1642, 1380, 1316, 1261 and 1020 cm^{-1}. The disagreement may be due to the different plants used in the study. However, the functional groups were obtained to act as the reducing agent (Aisida et al., 2021; Nindawat & Agrawal, 2019). In addition, the TEM result (Figure 3) revealed that the CAgNPs are spherical in shapes that facilitate the delivery of drugs to the target sites, as reported in the studies of Govindaraju et al. (2010); Saeed et al. (2020). The presence of silver as revealed by the EDS spectrum (Figure 3) in the characterized CAgNPs is similar to the results obtained by Samuggam et al. (2021); Srichaiyapol et al. (2021), in which silver was also present.

The results obtained for the rate of killing by the CAgNPs showed reductions in the populations of all the clinical bacterial isolates: *E. coli* strain MRE 600 (CP014197.1), *Salmonella enteric* subsp. Enteric serovar typhi PMO 16/13 (CP12091.1), *K. pneumoniae* strain HZW25 (CP025211.1) and *P. fluorescens* strain 2P24 (CP025542.1) between the periods of 1-7 h. These results were similar to the ones obtained in the studies of Betts et al. (2018); Smirnova and Oktyabrsky (2018); Srichaiyapol et al. (2021), in which there was a reduction in the population of the bacteria as the time of exposure increased. The value of $0.00 \log_{10}$cfu/ml was obtained at the sixth and seventh hours when *E. coli* strain MRE 600 (CP014197.1) was exposed to the CAgNPs, possibly showing the most significant bactericidal effect on *E. coli* strain MRE 600 (CP014197.1) followed by *Salmonella enteric* subsp. Enteric serovar typhi PMO 16/13 (CP12091.1) and bacteriostatic effect against *P. fluorescens* strain 2P24 (CP025542.1) and *K. pneumoniae* strain HZW25 (CP025211.1) Figure 5. There were increments in all the clinical bacterial isolates when exposed to the control between 1-7 h. This result is expected since the control did not contain CAgNPs.

5. CONCLUSION

The characterization and rate of killing of synthesized conjugated silver nanoparticles were carried out against selected clinical bacterial isolates. The CAgNPs have a bactericidal effect on *E. coli* strain MRE 600 (CP014197.1) and *Salmonella enteric* subsp. Enteric serovar typhi PMO 16/13 (CP12091.1) between 6-7 h exposures, respectively, which can be attributed to the properties of the CAgNPs. Therefore, the study suggests that the CAgNPs exhibit a strong antimicrobial activity and the potential to be developed as an alternative agent to treat bacterial infections, curb multidrug resistant bacterial infection, and further promote speedy drug delivery to the target sites.

CONFLICTS OF INTEREST

There is no conflict of interest among the authors.

ACKNOWLEDGMENTS

We want to thank Prof. Titilayo Akinlabi, VC of PAN African University, Ibadan, for her financial support characterising the conjugated silver nanoparticles in the University of Johannesburg, South Africa. Our gratitude also goes to the following people for the interpretation of the characterized conjugated silver nanoparticles: Dr. Oluwatosin Shittu, Head of Department, Department of Biochemistry, Federal University of Technology, Minna; Dr. Mercy Bankole and Dr. Tijani Jimoh, both of the Department of Chemistry, Federal University of Technology, Minna.

ORCID

Stephen Dare Oloninefa	0000-0001-9878-1906
Abalaka Moses Enemaduku	0000-0002-0006-9011
Daniyan Safiya Yahaya	
Mann Abdullahi	0000-0003-3241-3240

AUTHOR CONTRIBUTIONS

The authors provide equal contributions in: collection and/or assembly of data, data analysis and interpretation and writing the article.

REFERENCES

Aisida, S.O., Ugwu, K., Nwanya, A.C., Bashir, A.K.H., Nwankwo, N.U., Ahmed, I., Ezema, F.I., 2021. Biosynthesis of silver oxide nanoparticles using leave extract of Telfairia Occidentalis and its antibacterial activity. Materials Today: Proceedings. 36, 208–213. https://doi.org/10.1016/j.matpr.2020.03.005

Aritonang, H.F., Koleangan, H., Wuntu, A.D., 2019. Synthesis of Silver Nanoparticles Using Aqueous Extract of Medicinal Plants' (Impatiens balsamina and Lantana camara) Fresh Leaves and Analysis of Antimicrobial Activity. International Journal of Microbiology. 2019, 1–8. https://doi.org/10.1155/2019/8642303

Basappa, M.N., Subbaiah, V., Muthupalani, M., Yamagani, P.K., Mohan, K., Keshapaga, U.R., Asokan, S.V., Kalappurakkal, R.C., 2013. Antioxidant activity of carnosic acid and rosmarinic acid in raw and cooked ground chicken patties. Journal of the Science of Food and Agriculture, 23740828–23740828. https://doi.org/10.1002/jsfa.6248

Betts, J.W., Hornsey, M., Ragione, R.M.L., 2018. Novel Antibacterials: Alternatives to Traditional Antibiotics, Advances in Microbial

Physiology. Elsevier Ltd, pp. 123–169.
Cheesbrough, M., 2010. Laboratory Manual, District Laboratory Practice in Tropical Countries. Cambridge University Press, pp. 146–157.
Cheng, G., Dai, M., Ahmed, S., Hao, H., Wang, X., Yuan, Z., 2016. Antimicrobial drugs in fighting against antimicrobial resistance. Front. Microbiol. 7, 470–470. https://doi.org/10.3389/fmicb.2016.00470
Govindaraju, K., Tamilselvan, S., Kiruthiga, V., Singaravelu, G., 2010. Biogenic silver nanoparticles by Solanum torvum and their promising antimicrobial activity. Journal of Biopesticides. 3(1), 394–399.
Hugo, W.B., Russell, A.D., 2000. Determination of Rate of Killing, Pharmaceutical Microbiology. Blackwell Science, pp. 229–244.
Incorporation, B., 2012. Accuprep Genomic DNA Extraction Protocol and Accupower Hotstart PCR Protocol. www.bioneer.com
Incorporation, B.C., 2016. GenomeLabTM Dye Terminator Cycle Sequencing and DNA Clean Up for Sequencing Reaction and Protocol,. Kraemer Blvd, Brea, USA: 250 S, CA 92821, pp. 1–4. Availableatwww.beckmancoulter.com
Kalaichelvan, P.T., Manjumeena, R., Girilal, M., Mahesh, P., 2013. Augmenting potential antifungal activity of Gandhaka Rasayana (A siddha compound) using green conjugated silver nanoparticles from Couroupita guianensis leaf extract against selected pathogenic strains. International Research Journal of Pharmacy. 4(6), 234–239. https://doi.org/10.7897/2230-8407.04653
Kasthuri, J., Kathiravan, K., Rajendiran, N., 2009. Phyllanthin-assisted biosynthesis of silver and gold nanoparticles: a novel biological approach. Journal of Nanoparticle Research. 11(5), 1075–1085. https://doi.org/10.1007/s11051-008-9494-9
Lee, N.Y., Ko, W.C., Hsueh, P.R., 2019. Nanoparticles in the treatment of infections caused by multidrug-resistant organisms. Front. Pharmacol. 10, 1153–1153. https://doi.org/10.3389/fphar.2019.01153
Malawong, S., Thammawithan, S., Sirithongsuk, P., Daduang, S., Klaynongsruang, S., Wong, P.T., Patramanon, R., 2021. Silver Nanoparticles Enhance Antimicrobial Efficacy of Antibiotics and Restore That Efficacy against the Melioidosis Pathogen. Antibiotics. 10, 839–839. https://doi.org/10.3390/antibiotics10070839
Mcfarland, J., 1907. Nephelometer. Journal of the American Medical Association. 14, 1176–1178. https://doi.org/10.1001/jama.1907.25320140024001g
Murray, P.R., Baron, E.J., Jorgensen, J.H., Landry, M.L., Pfaller, M.A., 2007. Manual of Clinical Microbiology,. ASM Press, Washington DC, pp. 2082–2091.
Natan, M., Banin, E., 2017. From Nano to Micro: Using nanotechnology to combat microorganisms and their multidrug resistance. FEMS Microbiol. Rev. 41, 302–322. https://doi.org/10.1093/femsre/fux003
NCBI., 1988. Sequence BLAST. www.ncbi.nlm.nih.go
Nindawat, S., Agrawal, V., 2019. Fabrication of Silver Nanoparticles Using Arnebia Hispidissima (Lehm.) A. DC. Root Extract and Unravelling Their Potential Biomedical Applications. Nanomedicine, and Biotechnology. 47, 166–180. https://doi.org/10.1080/21691401.2018.1548469
Oloninefa, S.D., Abalaka, M.E., Daniyan, S.Y., 2020. Antibiotic Susceptibility Profile of Cronobacter sakazakii. Anchor University Journal of Science and Technology. 1(1), 10–15.
Saeed, S., Iqbal, A., Ashraf, M.A., 2020. Bacterial-mediated synthesis of silver nanoparticles and their significant effect against pathogens. Environ. Sci. Pollut. Res. 27, 37347–37356. https://doi.org/10.1007/s11356-020-07610-0
Samuggam, S., Chinni, S.V., Mutusamy, P., Gopinath, S.C.B., Anbu, P., Venugopal, V., Reddy, L.V., Enugutti, B., 2021. Green Synthesis and Characterization of Silver Nanoparticles Using Spondias mombin Extract and Their Antimicrobial Activity against Biofilm-Producing Bacteria. Molecules. 26, 2681–2681. https://doi.org/10.3390/molecules26092681
Sermakkani, M., Thangapandian, V., 2012. Biological Synthesis Of Silver Nanoparticles Using Medicinal Plant (Cassia italica) Leaves. International Journal of Current Research. 4(10), 53–058.
Siddiqi, K.S., Husen, A., Rao, R.A.K., 2018. A review on biosynthesis of silver nanoparticles and their biocidal properties. J. Nanobiotechnol. 16, 1–28. https://doi.org/10.1186/s12951-018-0334-5
Smirnova, G.V., Oktyabrsky, O.N., 2018. Relationship between Escherichia coli growth rate and bacterial susceptibility to ciprofloxacin. Federation of European Microbiological Societies Microbiology Letters. 365, 1–6. https://doi.org/10.1093/femsle/fnx254
Srichaiyapol, O., Thammawithan, S., Siritongsuk, P., Nasompag, S., Daduang, S., Klaynongsruang, S., Kulchat, S., Patramanon, R., 2021. Tannic Acid-Stabilized Silver Nanoparticles Used in Biomedical Application as an Effective Antimelioidosis and Prolonged Efflux Pump Inhibitor against Melioidosis Causative Pathogen. Molecules. 26, 1004–1004. https://doi.org/10.3390/molecules26041004
Xueting, Y., He, B., Liu, L., Qu, G., Shi, J., Hu, L., Jiang, G., 2018. Antibacterial Mechanism of Silver Nanoparticles in Pseudomonas Aeruginosa. Proteomics Approach. Metallomics. 10(4), 515–652. https://doi.org/10.1039/C7MT00328E